JMEPEG (2006) 15:675-683
DOI: 10.1361/105994906X150830

1059-9495/$19.00

Hole Expansion in a Variety of Sheet Steels

R.J. Comstock, Jr., D.K. Scherrer, and R.D. Adamczyk

(Submitted January 20, 2006)

Expanding pierced holes is a common forming practice and problems during these operations are not unusual. Adamczyk and Michal have previously developed an equation for maximum hole expansion of HSLA steels, for holes in the sheared then deburred condition. This paper expands the work of the above authors. Nineteen ferritic, ferritic stainless, and austenitic stainless steels were evaluated for hole expansion using various hole-edge conditions. It was found that the behavior of steels having finished holes is very different than those tested in the as-sheared condition. Relationships between hole expansion and tensile-mechanical properties were developed for both conditions.

Keywords forming, hole expansion, sheet steel, stretch flangeability

1. Introduction

Expanding pierced holes during flanging operations is very common in the automotive industry (Ref 1). During this procedure, a pierced hole is stretched with tension such that its diameter is increased. Often, these flanging operations stretch material that has already been subjected to large amounts of plastic deformation. Therefore, forming problems during the part-design phase, as well as during production, often result.

Early work had identified elongated inclusions as being detrimental to metalworking. In 1953, Van Vlack (Ref 2) suggested that silicon affected the distribution of inclusions, which controlled machinability. In 1955, E.J. Paliwoda (Ref 3) reported that oval, rather than stringer-like, globular sulfides are desirable for good machining properties. In 1965, Lichy et al. (Ref 4) investigated sulfide shape control in low-carbon Al-killed steel. These researchers found that zirconium inserted itself into the MnS precipitate, resulting in a nonductile sulfide. As a result, these sulfides maintained their globular shape after hot rolling. Aluminum and titanium were also studied but were not found to be effective in producing globular sulfides. Sims and Boulger (Ref 5) confirmed Lichy's results and reported similar resistance to sulfide deformation when selenium and tellurium are added, where these elements substitute for sulfur in the MnS precipitate. In 1970, Luyckx et al. (Ref 6) used the rare earth addition cerium for sulfide shape control in high strength low alloy (HSLA) steels. This resulted in significant improvements in both the transverse Charpy upper-shelf impact energy and the transverse formability during bending. This inclusion-deformation work eventually evolved into the use of tests designed to characterize the ability of a sheared hole to be expanded.

Hole expansion is generally measured using holes of diameter ~1 in. They are stretched using a hemispherical punch with failure being observed visually. Adamczyk et al. (Ref 1) used the above techniques in 1983 to measured hole expansion in a variety of steels, two of which were rare-earth treated for inclusion control. These rare-earth treated steels did not show significant variability in hole expansion between the as-sheared and sheared then deburred conditions. Most of the nontreated steel showed significant variations between the two conditions. Typically, hole expansion increases when the shear burr is removed because crack nucleation sites, as well as cold-worked material, are removed (Ref 1).

In 1986, Adamczyk and Michal (Ref 7) found that alloys using rare earth additions of lanthanum and cerium showed identical performance in hole-expansion tests using both as-sheared holes and sheared then deburred holes in HSLA steels. Alloys that were not rare earth treated showed poorer performance in the as-sheared condition. These researchers also found evidence of inclusions at crack initiation sites. A multiple regression analysis was used to develop the following equation for sheared then deburred holes:

$$\text{HE}\ (\%) = 1.7(r_{\text{m}})(e_{\text{t}(\%)}) + 15 \qquad \text{(Eq 1)}$$

where HE (%) is the percent of hole expansion, r_{m} is the average r value (plastic strain ratio), or simply the r value, given by Eq 2 (Ref 8-10):

$$r_{\text{m}} = \frac{r_0 + 2r_{45} + r_{90}}{4} \qquad \text{(Eq 2)}$$

where 0, 45, and 90 indicate the number of degrees from the rolling direction. In Eq 1, $e_{\text{t}(\%)}$ is the percent of transverse total elongation. The relationship in Eq 1 had an R^2 correlation coefficient of 0.968. Bhattacharya and Patil (Ref 11) also examined the effects inclusions had on edge formability of hot-rolled HSLA steel. These test results were very sensitive to the sulfur content, as hole-expansion performance decreased with increasing sulfur content. Low sulfur (<0.008 wt.%) and sulfides with low aspect ratios (globular shaped) led to the best edge formability using edge stretch tests (Ref 11).

As described above, edge formability and hole-expansion research has typically centered on controlling the shape and volume of sulfur inclusions. Low aspect ratio inclusions have been reported to narrow or eliminate the differences in hole expansion between sheared and finished holes (Ref 1, 7, 11). In addition, Adamczyk and Michal (Ref 7) developed an equation

R.J. Comstock, Jr. and D.K. Scherrer, AK Steel Corporation, Middletown, OH; and **R.D. Adamczyk**, AK Tube LLC, Wallbridge, OH. Contact e-mail: robert.comstock@aksteel.com.

Table 1 Sheet steels used in this study along with their mechanical properties, machined hole-expansion, and sheared hole-expansion results

Material(a)	Thickness, in.	Trans. YS, ksi	Trans. TS, ksi	Trans. *n* value	Trans. total elong., %	Avg. r_m	Sample ID	Machined holes		Sheared holes		
								Avg. HE, %	Std. dev.	Avg. HE, %	Std. dev.	Best die condition
Ferritic Steels												
ULTRA FORM 409	0.057	33.6	60.9	0.229	36	1.60	1	128	2	Not tested	…	…
HIGH PERFORMANCE-10 409	0.057	33.2	59.3	0.230	37	1.53	2	118	5	101	0.8	0.755 down
HIGH PERFORMANCE-10 409	0.059	42.8	59.4	0.187	33	1.28	3	Not tested	…	79	3	0.755 up
MD-3 409	0.059	38.4	58.3	0.211	36	1.31	4	81	2	75	0.5	0.767 up
ULTRA FORM 439	0.058	48.7	66.0	0.182	34	1.75	5	Not tested	…	118	8	0.762 up
HIGH PERFORMANCE-10 439	0.057	41.1	64.4	0.210	36	1.61	6	106	4	Not tested	…	…
18 SR	0.057	56.3	76.7	0.182	31	1.10	7	75	9	79	5	0.762 up
18 Cr-Cb	0.062	46.2	68.9	0.195	36	1.30	8	100	2	80	9	0.767 up
IF	0.056	19.2	43.6	0.237	47	1.86	9	Not tested	…	131	11	0.755 and 0.762 up
HIGH PERFORMANCE-10 409	0.046	42.5	61.2	0.199	36	1.49	10	103	3	Not tested	…	…
HIGH PERFORMANCE-10 439	0.022	43.4	67.6	0.205	29	1.45	11	59	5	Not tested	…	…
18 Cr-Cb	0.024	50.9	70.7	0.178	29	1.65	12	82	2	Not tested	…	…
18 Cr-Cb	0.047	52.8	70.0	0.166	33	1.58	13	108	4	Not tested	…	
IF	0.043	19.3	41.8	0.240	49	1.74	14	201	5	Not tested	…	…
Al ULTRA FORM 409	0.028	41.4	66.3	0.179	31	1.48	15	92	6	Not tested	…	…
Austenitic Steels												
304L	0.058	40.7	88.5	0.406	53	0.94	16	158	11	33	2	0.755 up
304L	0.059	46.9	95.8	0.471	54	1.02	17	Not tested	…	66	0.5	0.767 up
NITRONIC 30	0.060	59.8	113.2	0.406	52	1.00	18	Not tested	…	39	0.8	0.767 up
NITRONIC 30	0.020	54.8	115.2	0.448	58	1.05	19	121	4	Not tested	…	…

(a) ULTRA FORM, HIGH PERFORMANCE-10, 18 SR, 18 Cr-Cb, and NITRONIC are trademarks of AK steel Corporation.

(Eq 1) for HSLA steels with sheared then deburred (finished) holes that describes hole expansion in terms of the average *r* value and the transverse total elongation. The current work develops a similar relationship over a wider range of sheet steels that include interstitial-free (IF) as well as austenitic and ferritic stainless steels, for both finished holes and holes in the as-sheared condition. The results of this study are presented below.

2. Experimental Procedures

2.1 Materials

A variety of sheet steel products were used in this study to get a large spread in mechanical properties. Table 1 lists each sheet steel product, its thickness, the transverse mechanical properties, and *r* values. Material ID numbers are also assigned in Table 1 to clearly convey which material was used in each test, as testing of all materials under all conditions was not possible.

As discussed in the Introduction, elongated inclusions have a negative impact on hole expansion. None of the products tested exhibited elongated inclusions when viewed in the as-polished condition in the longitudinal direction with an optical microscope. Rather than show a micrograph for each steel, Fig. 1 shows representative unetched longitudinal micrographs for a few of the steels.

2.2 Hole-Expansion Testing

Except where otherwise noted, the following procedures were used in the hole-expansion testing:

- Blanks were cut into 7 × 7 in. samples, and a hole was fabricated in the center.
- Samples were degreased with ethanol.
- An MTS limiting dome height (LDH) tester (MTS Systems Corporation, Eden Prairie, MN) was used on the hole-expansion setting with a 4 in. diameter ball.
- The punch and dies were degreased with ethanol before each set of tests.
- Ferrocote 61 (Quaker Chemical Corporation, Conshohocken, PA) MAL-HCL-1 lubricant was brushed on the punch prior to each test.
- Failure was determined visually and was defined as fracture or severe necking; a flashlight was used to illuminate the sample.

The LDH tester has lockbeads in the hold-down die and uses a 60,000 lb hold-down force to prevent draw-in. The punch rate in the hole-expansion setting is 0.02 in./s. The punch travel can be temporarily paused to allow for closer examination of the circumference of the hole during testing. The test was terminated when a visible crack was observed (Ref 12). Due to the subjective nature of defining failure, the same operator (the author, R.J.C.) carried out all testing reported in Table 1 in an attempt to provide as consistent results as possible.

2.3 Machined Holes

The effect of finished holes on hole expansion was investigated using 1.5 in. diameter machined holes in HIGH PERFORMANCE-10 409 at 0.057 in. thick (material ID 2). This material was tested in two conditions. In the first, the holes

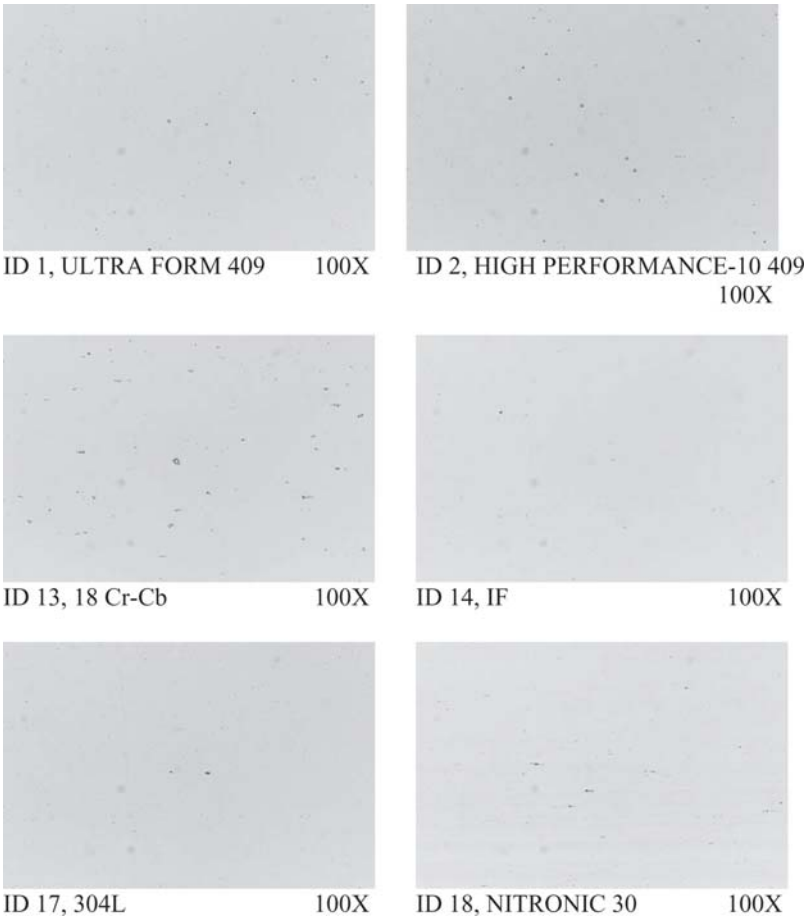

Fig. 1 Representative unetched longitudinal micrographs for some of the steels listed in Table 1

were fabricated using a milling machine. In the second, the milled holes were then sanded using first 500 and then 1000 grit paper. Figure 2 shows examples of each of these two types of hole finishes.

Testing was conducted using the procedures specified above using four samples in each condition. The average hole expansion of the machined holes was 115% (standard deviation of 6%), and the average of the machined and sanded holes was 119% (standard deviation of 4%). The similarity of these results indicates that the machined holes are of high quality and insensitive to subtle changes in their surface characteristics.

Use of a 1.50 in. diameter hole in the above tests resulted in failure diameters approaching 3.5 in. The diameter of the punch is 4 in. A smaller initial hole diameter was required to successfully test more ductile material. Therefore, the diameter of the machined holes was reduced to 0.750 in. The same material (ID 2) was tested again with machined, 0.750 in. diameter holes. The hole expansion was measured to be 118% (standard deviation of 5%). This is nearly identical to the 115% average hole expansion (standard deviation of 6%) measured for the machined 1.5 in. diameter holes. Changing the hole diameter by a factor of 2 does not influence the results in this hole-expansion test. This is in agreement with the work of Davies (Ref 12), who reported that varying the sheared hole diameter between 0.375 and 0.500 in. resulted in no discernible difference in hole expansion for high-strength steels. Samples with milled 0.750 in. diameter holes were used for the remainder of testing. The condition of these holes is identical to that of the 1.50 in. diameter hole illustrated in Fig. 2(a). All holes were evaluated before testing using a stereomicroscope to ensure good quality.

The one exception to the above hole-testing procedure occurred during the testing of the 0.058 in. thick 304L material (ID 16). This was the only heavier gage austenitic stainless steel tested in the machined-hole condition. The failure loads exceeded those that could be obtained by the MTS LDH tester, which has a 30,000 lb maximum load capability. Therefore, these tests were run on the Interlaken Formability Press at AK Steel Corporation, which has a 120,000 lb load capability. Due to the different configuration of the Interlaken Press, failure was determined using the load-drop method. In addition, the Ferricote FC 61 lubricant proved inadequate at these higher loads, and stick-slipping conditions occurred during preliminary tests. Therefore, a lubricant designed for higher loads, Klenedraw (Tower Oil, Chicago, IL), was used at full concentration for the 0.058 in. thick 304L (material ID 16) machined-hole tests.

2.4 Sheared Holes

Sheared 0.750 in. diameter holes were produced using tooling designed and fabricated at AK Steel Corporation. Sheared holes were produced using a 0.750 in. diameter punch with interchangeable circular dies in five sizes ranging from 0.755 to 0.773 in. in diameter. Some researchers report that die clearance has a significant impact on the characteristics of sheared holes (Ref 13). Davies (Ref 12), however, conducted hole-expansion tests on high-strength steels with holes sheared using die clearance between 2 and 20% of the sheet thickness. This

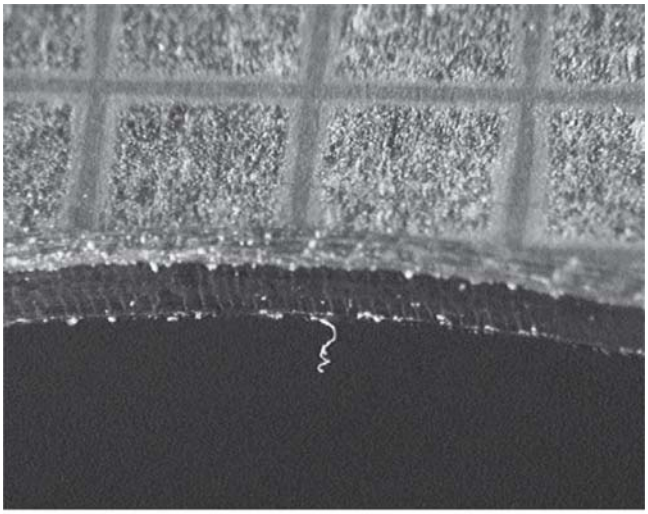

(a)

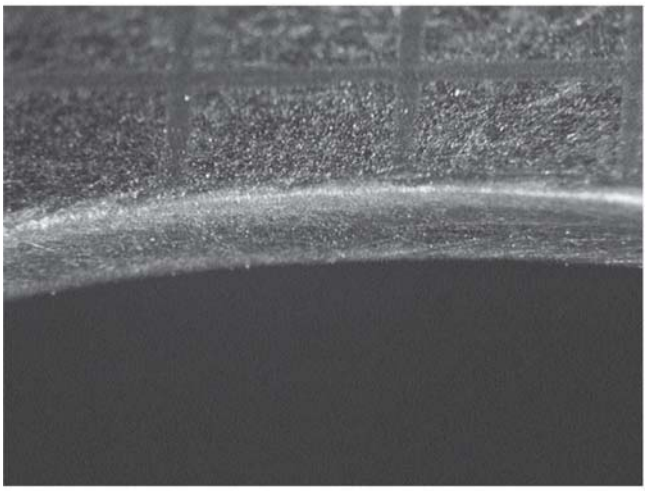

(b)

Fig. 2 Surface characteristics of (a) machined and (b) machined and finished (with 500 and then 1000 grit paper) 1.50 in. diameter hole in ID 2 material (grid spacing = 0.10 in.)

variation did not affect the ratio of sheared to fracture surface and was reported to not have an influence on hole expansion. In any event, sheared holes having about 5, 10, 15, and 20% clearance were tested. The die clearance (C_D) is described as the distance between the punch and die, expressed as a percent of the sheet thickness (Ref 13). The die clearances calculated for this work were determined using the assumption that the punch was perfectly centered with the die. The die clearance can then be determined using the following equation:

$$C_D = \frac{(D_{Die} - D_{Punch})}{2 \cdot t} \cdot 100\% \quad \text{(Eq 3)}$$

where D is the diameter of either the die or the punch and t is the sheet thickness. All sheared holes were inspected using a stereomicroscope to insure that the above assumption was reasonable and that the sheared holes were of high quality and reasonably symmetric, as illustrated in Fig. 3.

2.5 Determination of the Percent Hole Expansion

The percent hole expansion, HE (%), was determined by testing a minimum of three samples in each condition. The diameter of the initial hole was measured, using calipers, prior to testing. The diameter of the expanded hole, after failure, was determined by taking the average of the expanded-hole diameter in four directions: the longitudinal, transverse, and the two diagonal directions. If a crack occurred in one of these directions, the measurement was offset slightly so as to not include the crack. The percent hole expansion was determined using the following equation (Ref 1, 7, 10-12, 14, 15):

$$\text{HE}\ (\%) = \frac{(D_f - D_i)}{D_i} \cdot 100\% \quad \text{(Eq 4)}$$

where D_f and D_i are the final and initial hole diameters, respectively.

3. Results and Discussion

3.1 Strain Distribution Results

Samples of 18 Cr-Cb (material ID 13) and IF steel (material ID 14) each had a strain grid applied. Holes having a diameter of 0.750 in. were machined, and the samples were strained to failure. In both cases, the minor strain was negative from the hole edge to a distance of ~1/2 in. away from the edge. The strain state then transitions to a ring of plane strain deformation. This is in agreement with the strain analysis of previous workers (Ref 7). Near the edge, the ratios of major to minor strain are −3 and −6 for 18 Cr-Cb and IF steel, respectively. The absolute value of this ratio is above those measured for ferritic steels in uniaxial tension, −2. Therefore, the strain state at the hole edge is between uniaxial tension and plane strain. This strain state is expected to yield lower failure strains than the total elongation observed in a uniaxial tensile test when viewed with respect to typical forming limit diagrams (Ref 8). Therefore, the strain state at the hole edge does not explain the high forming limits of some expanded holes. It is theorized that the added formability is due to material near the hole edge being constrained by the adjacent material having a lower strain level.

3.2 Machined Hole Expansion Results

Samples with 0.750 in. diameter machined holes were prepared and tested using the procedures described above. These hole-expansion results are given in Table 1. Not all of the materials listed were tested under this condition. A regression analysis was conducted. These results are plotted in Fig. 4. The material having the highest measured hole expansion, the IF steel (material ID 14), is highlighted. This is the furthest outlying point in the regression analysis.

The results of the linear regression analysis illustrate that the material thickness, average r value, and total elongation allow for the hole expansion to be calculated over a wide variety of steels. The resulting equation of the regression analysis is given in Eq 5:

$$\text{HE}\ (\%) = 478t + 2.56e_{t(\%)} + 35.3r_m = 58.2 \quad \text{(Eq 5)}$$

where t is the thickness in inches, $e_{t(\%)}$ is the total transverse elongation for a 2 in. gauge section (in percent), and r_m is the average r value. The R^2 term is 0.83 when the data is fit through the origin with a slope of one, which is the expected

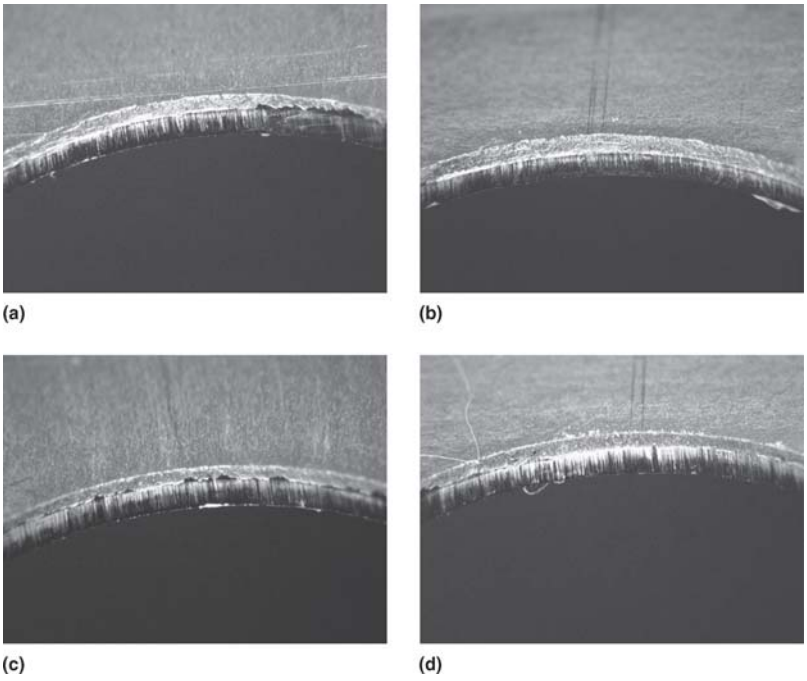

Fig. 3 Example of a sheared hole at (a) 0°, (b) 90°, (c) 180°, and (d) 270° from the rolling direction produced with the shear-hole tooling used at AK Steel Corporation's Interlaken Formability Press

slope when calculated values are plotted against experimental ones.

Also shown in Fig. 4, as open triangles, are the experimental results of Adamczyk and Michal (Ref 7). Adamczyk and Michal tested HSLA material with sheared holes that were deburred prior to testing. Therefore, their data is comparable to the machined hole data reported here. Table 2 lists the mechanical properties and measured hole expansion results of Adamczyk and Michal. Two steels that did not have a fully recrystallized structure are denoted "RA" for recovery annealed. In all, data from 22 steel-thickness combinations having measured hole expansions from 24 to 149% are plotted in Fig. 4.

Equation 5 indicates that nearly 5 percentage points in hole expansion are gained for every 0.010 in. increase in thickness. Two percentage points in hole expansion are gained for every 1% increase in the measured transverse elongation, and 3.5 percentage points are gained for every 0.1 increase in the average *r* value.

Adamczyk and Michal had previously shown good agreement between the average *r* value and transverse total elongation for HSLA and recovery-annealed steels (Ref 7). Figure 5 replots the results of Tables 1 and 2 using the relationship determined by Adamczyk and Michal. This relationship was previously given as Eq 1.

Figure 5 shows that this relationship also fits quite well for the machined hole data having a correlation coefficient of 0.84 and a slope of 1.2. The only outlying points are those of IF steel (material ID 14) and 304 (material ID 16). Note that this relationship is independent of thickness. Inclusion of the thickness term in Eq 5 does not significantly improve the fit with the measured hole-expansion data. However, Eq 1 is improved slightly when running the regression analysis over the full data set given in Tables 1 and 2. The correlation coefficient is still 0.84, but the slope is equal to 1.0. These results are given as Eq 6 and plotted in Fig. 6:

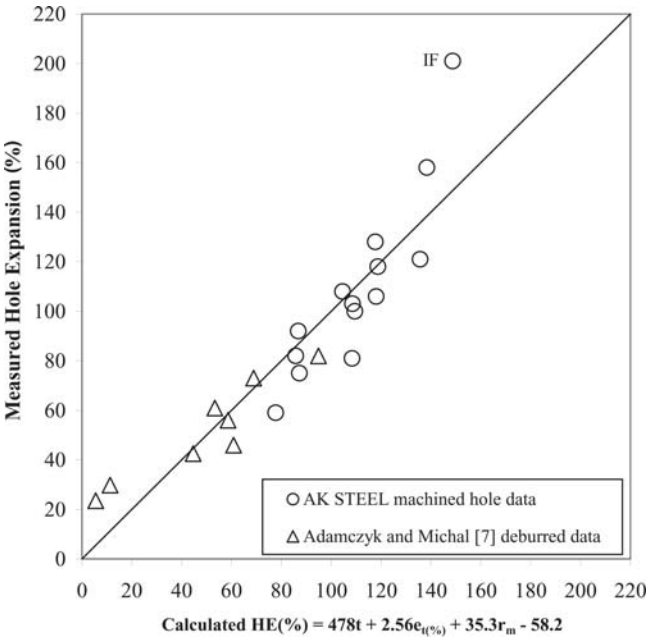

Fig. 4 Hole-expansion results for machined holes using Eq 5. The circles are the results of this work for the steels listed in Table 1. The data point having a measured hole expansion of 201 is for the IF steel material (ID 14). Also shown are the experimental results of Adamczyk and Michal (Ref 7), Table 2, plotted using the regression analysis equation given above.

$$\text{HE}\ (\%) = 2.0(r_m \times e_{t(\%)}) + 5.5 \qquad \text{(Eq 6)}$$

It is clear from Fig. 4 and 6 that Eq 5 and 6 both do a good job of predicting the hole-expansion behavior in finished holes from the mechanical properties of the combined sets of data of Tables 1 and 2. Equation 6 does this without introducing a

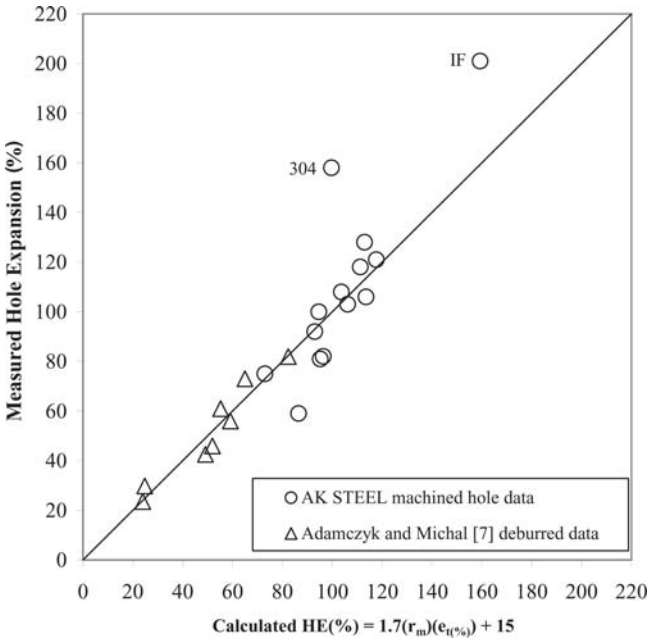

Fig. 5 Hole-expansion results for machined holes using the previous developed equation, Eq 1, of Adamczyk and Michal (Ref 7)

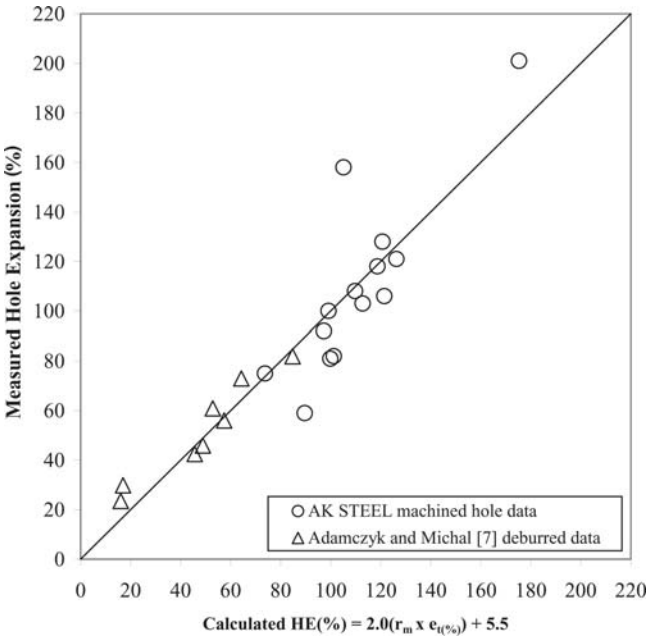

Fig. 6 Refinement of Adamczyk and Michal's function predicting hole expansion (Ref 7), given in Eq 6

Table 2 Mechanical properties and measured hole expansion for tests conducted by Adamczyk and Michal in the sheared then de-burred condition

		Transverse mechanical properties				
Material	**Thickness, in.**	**YS, ksi**	**TS, ksi**	**Elongation, %**	**Average *r* value**	**Average HE, %**
HSLA 35	0.044	38.0	56.7	36.7	1.08	81.9
HSLA 45	0.028	53.6	60.1	22.8	0.88	42.5
HSLA 50 #1	0.031	59.1	72.7	24.4	0.97	60.9
HSLA 50 #2	0.031	61.4	69.3	26.2	0.99	56.0
HSLA 50 #3	0.031	56.5	65.7	30.6	0.96	73.0
HSLA 60	0.057	73.0	84.7	22.6	0.96	45.9
RA 70	0.05	75.0	79.1	8.3	0.69	29.8
RA 80	0.042	81.5	86.1	8.5	0.62	23.5

Source: Ref 7

thickness term, only the average *r* value and transverse total elongation are used, whereas Eq 5 uses all three properties. Figures 5 and 6 also underline the quality of the function initially formulated by Adamczyk and Michal in 1986 (Ref 7).

Common in Eq 1, 5, and 6 is the positive impact that both the average *r* value and the transverse total elongation have on the hole-expansion behavior of machined holes. The *r* value is commonly described as the resistance to thinning for sheet metals. This is because the *r* value relates the change in width and the change in thickness that results from an applied tensile strain (Ref 8-10):

$$r = \frac{\varepsilon_w}{\varepsilon_t} \quad \text{(Eq 7)}$$

where ε_w and ε_t are the strains in the width and thickness directions, respectively. An expanding hole will only fail after it becomes unstable against thinning. One would expect the *r* value to positively impact edge formability (Ref 7).

It is also of no surprise that the total transverse elongation would scale with the amount a hole can be successfully expanded. The transverse elongation may capture the decreases in ductility caused by various inclusions, including those that are elongated (Ref 7). The thickness term that shows up in Eq 5 is also not unexpected. The formability of sheet steel in plane strain, FLD_0, is predicted to increase with increasing sheet thickness (Ref 9, 16).

3.3 Sheared Hole Expansion Results

Three steels were tested in both the burr-up and burr-down positions using the 0.750 in. diameter punch and four die diameters: 0.755, 0.762, 0.767, and 0.773 in. These correspond roughly to die clearances of approximately 5, 10, 15, and 20%. Figure 7 shows the results of the best clearance condition for both burr orientations. These conditions are reported in Table 1. The HIGH PERFORMANCE-10 409 (material ID 2) and 304L (material ID 16) results are similar, but the 18 SR (ID 7) results are slightly better for the burr-up condition. This seems reasonable, as burr-down material would experience further deformation of the burr due to contact with the punch. To reduce sample preparation and testing time, the rest of the

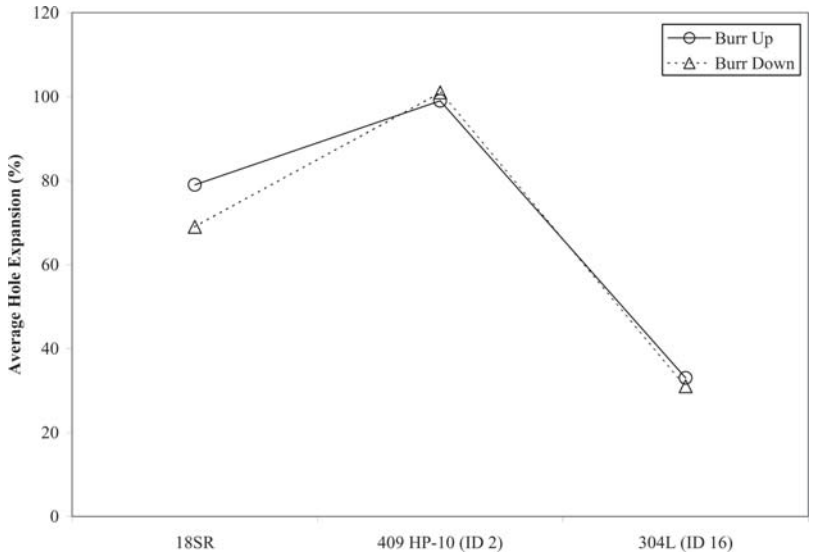

Fig. 7 Results of the best die clearance condition for both the burr-up and burr-down orientations for HIGH PERFORMANCE-10 409 material (ID 2), 304L (ID 16), and 18 SR (ID 7) alloys

samples were tested in the burr-up orientation with holes sheared using each of the four die diameters listed above. The best die clearance condition, as described in Table 1, was used in the following analysis.

Table 1 gives the experimental results of the sheared hole-expansion tests. The sheared hole-expansion results are an average of three tests in all cases except for two. The IF (material ID 9) and 304L (material ID 16) both had an average of five tests. Note that all samples tested were at approximately the same thickness, in the range from 0.057 to 0.062 in.

Regression analysis using the sheared-hole data in Table 1 yielded the following equation:

$$\text{HE}\ (\%) = 85.7r_{\text{m}} - 31.4n_{\text{t}} - 23.6 \qquad \text{(Eq 8)}$$

where r_{m} is the average r value and n_{t} is the work-hardening rate for a transverse tensile test from 10% engineering strain to the strain at the maximum uniform elongation. The results are plotted in Fig. 8 as open circles. Figure 8 shows that Eq 8 does a good job in predicting the hole-expansion behavior for this sheared-hole data. The correlation coefficient is 0.91 with a slope of 1.0.

Additional data were available from AK Steel Corporation for austenitic stainless steels at a thickness of ~0.020 in. Details are given in Table 3. Holes were sheared using the shear-hole tooling with the 0.750 in. diameter punch and the 0.755 in. diameter die. Hole expansion was determined using an average of five tests. Hole expansion predicted using Eq 8 and the measured-hole expansion are also plotted in Fig. 8 as open triangles. Equation 8 also predicts well the hole-expansion behavior of sheared holes for these thinner austenitic stainless steels.

Five materials were tested in both the machined and sheared condition. The percent decrease between the machined hole expansion and the sheared hole expansion is very dependent on the work-hardening exponent (n_{t}), as illustrated in Fig. 9. This behavior is expected as higher work-hardening rates will result in higher strength material at the sheared edge (Ref 1). For a given material class, fracture toughness generally decreases as

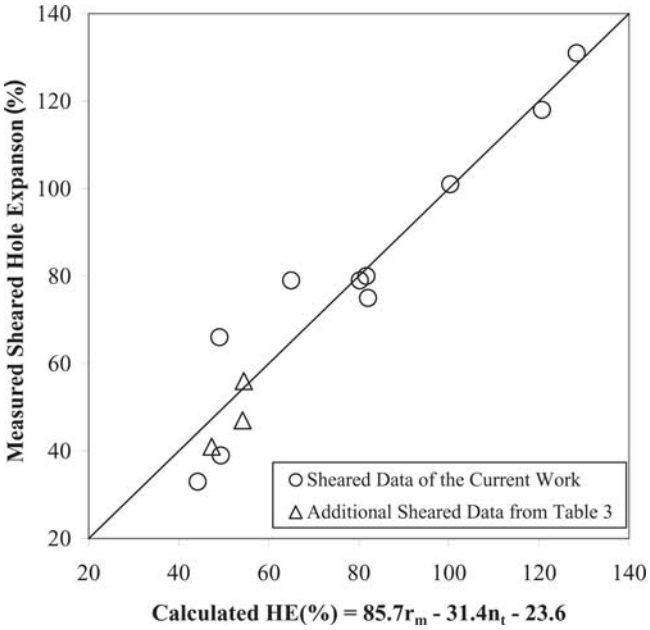

Fig. 8 Sheared-hole expansion results predicted by Eq 8 are compared with average experimental values for the steels listed in Table 1. Also plotted are additional hole-expansion data measured from three austenitic stainless steels at ~0.020 in. thick, listed in Table 3.

the material strength increases (Ref 17, 18). In addition, sheared holes are expected to created more fracture nucleation sites than machined holes (Ref 1).

Adamczyk and Michal (Ref 7) found that alloys using rare earth additions of lanthanum and cerium showed identical performance in hole-expansion tests using both as-sheared holes and sheared then deburred holes in HSLA steels. The work-hardening exponent for HSLA steels is generally below 0.2. This was the case in the above work. The low work-hardening rates of ferritic steels is shown to result in minimal differences between the machined and sheared hole expansions for inclusion-controlled material. This is in agreement with the results of Adamczyk and Michal (Ref 7).

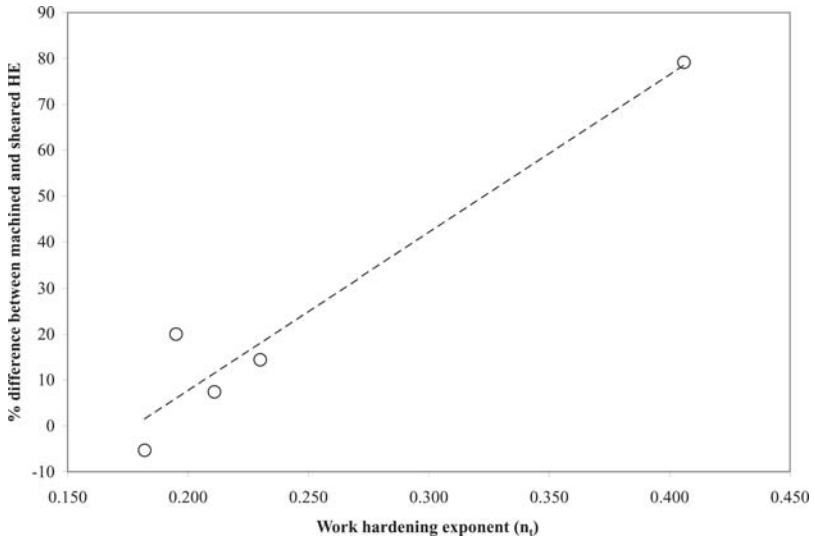

Fig. 9 Percent difference between machined and sheared hole expansion as a function of the transverse work-hardening exponent

Table 3 Additional AK Steel sheared hold-expansion results for three austenitic stainless steels (averages are from five tests)

Material	Thickness, in.	Trans. YS, ksi	Trans. TS, ksi	Trans. *n* value	Avg. *r* value	Avg. hole expansion, %
304	0.020	43.9	120.2	0.580	1.04	41
304L	0.017	45.0	99.5	0.443	1.07	47
316	0.020	37.8	88.6	0.462	1.08	56

5. Conclusions

- Changing the hole diameter by a factor of 2 (from 1.50 to 0.750 in.) does not influence the hole-expansion results using machined holes. This is in agreement with the work of Davies (Ref 12), who reported that varying the sheared hole diameter between 0.375 and 0.500 in. resulted in no discernible difference in hole expansion for high-strength steels.
- Hole expansion of machined, or finished, holes is predicted fairly well for most steels using the relationship described by Adamczyk and Michal (Ref 7) (Eq 1, repeated below):

$$\text{HE}\ (\%) = 1.7(r_{\text{m}} \times e_{\text{t}(\%)}) + 15$$

The predictive capability of this relationship was improved by running a regression analysis that included current data from AK Steel Corporation (Eq 6, repeated below):

$$\text{HE}\ (\%) = 2.0(r_{\text{m}} \times e_{\text{t}(\%)}) + 5.5$$

Including the thickness in the regression analysis does not improve it but provides equivalent predictive results as Eq 6. This relationship is given as Eq 5 (repeated below):

$$\text{HE}\ (\%) = 478t + 2.56e_{\text{t}(\%)} + 35.3r_{\text{m}} - 58.2$$

- Regression analysis of the hole-expansion of sheared holes in the best die clearance condition yielded an equation (Eq 8, repeated below), quite different than those of the machined holes:

$$\text{HE}\ (\%) = 85.7r_{\text{m}} - 31.4n_{\text{t}} - 23.6$$

This equation underlines the detrimental effect that cold-worked edges have on their ability to deform.

- The difference between machined hole and sheared hole expansion is dependent on the work-hardening rate. Higher *n* values result in the sheared holes performing worse than machined holes.

References

1. R.D. Adamczyk, D.W. Dickinson, and K.P. Krupitzer, The Edge Formability of High-Strength Cold-Rolled Steel, 1983, SAE Paper 830237
2. H. Lawrence and V. Vlack, Correlation of Machinability with Inclusion Characteristics in Resulphurized Bessemer Steels, *Trans. ASM,* 1953, **45,** p 741-757
3. E.J. Paliwoda, The Influence of Chemical Composition on the Machinability of Rephosphorized Open Hearth Screw Steel, *Trans. ASM,* 1955, **47,** p 680-691
4. E.J. Lichy, G.C. Duderstadt and N.L. Samways, Control of Sulfide Shape in Low Carbon Al-Killed Steel, *J. Metals,* 1965, p 769-775
5. E.C. Sims and F.W. Boulger, Discussion of Control of Sulfide Shape in Low Carbon Al-Killed Steel, *J. Metals,* 1965, p 775
6. L. Luyckx, J.R. Bell, A. McLean, and M. Korchynsky, Sulfide Shape Control in High Strength Low Alloy Steels, *Met. Trans.,* 1970, **1,** p 3341-3350
7. R.D. Adamczyk and G.M. Michal, Sheared Edge Extension of High-Strength Cold-Rolled Steels, *J. Appl. Metalwork.,* 1986, **4**(2), p 157-163
8. E.G. Dieter, *Mechanical Metallurgy,* 3rd ed., McGraw-Hill, 1986, p 671-675
9. W.F. Hosford and R.M. Caddel, *Metal Forming: Mechanics and Metallurgy,* Prentice-Hall, 1983, p 264-265, 299-302

10. B. Taylor, Formability Testing of Sheet Metals, *Metals Handbook, Vol 14, Forming and Forging,* 9th ed., ASM, 1988, p 877-899
11. D. Bhattacharya and R.S. Patil, Edge Formability Properties of a Hot Rolled HSLA Steel Desulfurized by Various Methods, ASM Paper 8306-085, ASM, 1984, p 429-441
12. R.G. Davies, Edge Cracking in High Strength Steels, *J. Appl. Metalwork.,* 1983, **2**(4), p 293-299
13. Piercing of Low-Carbon Steel, *Metals Handbook, 9th ed., Vol. 14, Forming and Forging,* ASM, 1988, p 459-471
14. F.-L. Cheng and D. Aichbhaumik, The Effect of Hot-Dipped Galvanized Coating on the Edge and Plane Strain Formabilities of High Strength Steels, *J. Appl. Metalwork.,* 1986, **4**(2), p 176-182
15. K.-I. Sugimoto, K. Nakano, S.-M. Song, and T. Kashima, Retained Austenite Characteristics and Stretch-Flangeability of High-Strength Low-Alloy TRIP Type Bainitic Sheet Steels, *ISIJ Int.,* 2002, **42**(4), p 450-455
16. P. Stuart, X. Keeler, and W.G. Brazier, Relationship Between Laboratory Material Characterization and Press-Shop Formability, *Micro-Alloying,* 1977, **75,** p 517-530
17. H.T. Courtney, *Mechanical Behavior of Materials,* McGraw-Hill, Inc., 1990, p 480
18. V.F. Zackay, E.R. Parker, J.W. Morris, Jr., and G. Thomas, The Application of Materials Science to the Design of Engineering Alloys: A Review, *Mater. Sci. Eng.,* 1974, **16,** p 201-221